Width of Homopolymer Interfaces in the Presence of Symmetric Diblock Copolymers

T. P. Russell* and A. Menelle

IBM Research Division, Almaden Research Center, 650 Harry Road, San Jose, California 95120-6099

W. A. Hamilton and G. S. Smith

Los Alamos National Laboratory, Los Alamos, New Mexico 87545

S. K. Satija and C. F. Majkrzak

Reactor Radiation Division, National Institute of Standards and Technology, Gaithersburg, Maryland 20899

Received March 4, 1991; Revised Manuscript Received May 30, 1991

ABSTRACT: The interface between polystyrene and poly(methyl methacrylate) homopolymers was investigated as a function of the concentration of added symmetric diblock copolymer of PS and PMMA, denoted P(S-*b*-MMA), using neutron reflectivity. It was found that as the number of P(S-*b*-MMA) chains added to the interface between PS and PMMA was increased, the width of the gradient between the PS and PMMA segments broadened. In particular, the width of the interface between PS and PMMA homopolymers is 50 Å and, with the addition of P(S-*b*-MMA), increases to ~85 Å. At an amount corresponding to approximately half the thickness of the lamellar microdomain periodicity in the bulk, the interface becomes saturated with the copolymer. Further addition of copolymer chains to the interface results in a marked increase in the off-specular scattering, which is associated with either an ordering of the copolymer chains at the interface or an increase in the curvature of the interface. Studies were also performed on mixtures of homopolymers and copolymers. Here, the interface between the lamellar microdomains of the P(S-*b*-MMA) is found to increase from 50 Å for the pure copolymer to 75 Å as PS and PMMA homopolymer is added to the copolymer. The broadening of the interface seen in both sets of experiments is due to a significant penetration of the homopolymer into the interfacial region. These results are consistent with the reduction in the interfacial tension between the homopolymers with the addition of the diblock copolymer.

Introduction

The extent to which immiscible polymers mix at an interface depends upon the segmental interaction parameter and the statistical segment lengths of the polymers. The more favorable the interactions between the segments, the larger the extent of interpenetration of the segments will be. For a constant segmental interaction, the larger the statistical segment length, the broader will be the interface formed between the two polymers. Numerous theoretical treatments have appeared in the literature treating the interfacial characteristics of two immiscible polymers.[1-10] Experimentally, however, the investigation of the interface requires techniques that can probe the variation in the segment densities or concentrations over size scales that are less than the size of the molecules. Small-angle X-ray and neutron scattering techniques have been used in the past where the scattered intensity at high scattering vectors is damped according to the magnitude of the interface formed between the phases. However, there are severe limitations on the precision to which the interface can be measured by scattering techniques since the scattering is inherently weak and subtraction of the scattering associated with thermal density fluctuations is often of the same magnitude as the coherent scattering of interest. Recently, dynamic secondary ion mass spectrometry[11-13] and neutron reflectivity[14-17] have emerged as techniques with the spatial resolution comparable to or less than the size of polymer chains, and, consequently, quantitative examination of the interfacial behavior is now possible. In cases where the interaction parameter and statistical segment lengths are known, the experimentally measured interfacial widths are much larger than theoretical predictions. Nonetheless, the interface between immiscible polymers is small. This translates into a limited amount of segmental interpenetration and weak adhesion between the two polymers.[18]

One means by which the adhesion between immiscible polymers can be improved is by the use of diblock copolymers.[18,19] In this case one of the blocks preferentially resides in one of the homopolymers and the other block in the second homopolymer. Thus, the diblock copolymer forms a bridge between the two homopolymers, thereby improving adhesion. The behavior of diblock copolymers at the interface between immiscible polymers has been treated theoretically with specific predictions as to the segment density profiles of the homopolymers and copolymers at the interface. As with the simple homopolymer interface question, the number of experimental efforts dealing with this problem has been limited by the resolution capabilities of the techniques available. In an elegant electron microscopy study Jérôme et al.[19] were able to show that diblock copolymers preferentially segregated to the interface. More recent studies using forward recoil spectrometry,[20] dynamic secondary ion mass spectrometry,[21,22] neutron reflectivity,[23] and electron microscopy[24] have provided a more quantitative picture of the interfacial behavior of diblock copolymers.

In this article the effect on the interface between immiscible homopolymers of polystyrene, PS, and poly(methyl methacrylate), PMMA, is examined as a function of the amount of the corresponding diblock copolymer, denoted P(S-*b*-MMA), introduced to the system. It is shown that as the amount of copolymer is increased the interface between the PS and PMMA segments broadens. This broadening continues up to a point where the interface becomes saturated with the diblock copolymer. As the amount of copolymer at the interface is increased beyond this saturation point, the copolymer begins to form ordered structures or develops marked curvature. In addition, it is shown that the addition of homopolymers to P(S-*b*-MMA) results in a broadening of the interface between the PS and PMMA lamellar microdomains. This broad-

0024-9297/91/2224-5721$02.50/0

Table I
Homopolymer and Copolymer Characterization

polymer	M_{PS}	M_{PMMA}	M_w/M_n
P(S-*b*-MMA)	57 800	56 100	1.10
P(d-S-*b*-MMA)	52 900	48 000	1.07
P(S-*b*-d-MMA)	56 300	65 000	1.12
PS	127 000		1.05
d-PS	110 000		1.05
PMMA		107 000	1.05
d-PMMA		146 000	1.04

ening increases as the concentration of the homopolymer is increased. The broadening seen in both the homopolymer and copolymer interfaces is a direct consequence of the extent to which the homopolymer penetrates into the interfacial region.

Experimental Section

The characteristics of the homopolymers and diblock copolymers used in this study are given in Table I. The materials were purchased from Polymer Laboratories Ltd. The homopolymers were used as received, whereas the P(S-*b*-MMA) was thoroughly rinsed in cyclohexane to remove residual PS homopolymer prior to use. Size-exclusion chromatography was used to characterize the molecular weights of all the polymers.

Specimens for the neutron reflectivity studies were prepared in two different ways. For the studies on the copolymer at the interface between the PS and PMMA homopolymers, a film of d-PMMA was spin coated onto a Si substrate from a toluene solution. The solution concentration was adjusted to yield a d-PMMA film thickness of approximately 1×10^3 Å. A separate film of P(S-*b*-d-MMA) was spin coated onto a microscope slide. The sides of the slide were scored with a razor blade, and the film was floated off onto a pool of deionized water. The d-PMMA-coated substrate was then used to retrieve the P(S-*b*-d-MMA) film floating on the water. This bilayer was then dried at 80 °C for 20 min. A film of PS was then prepared on a microscope slide, floated off onto deionized water, and retrieved with the bilayer-coated substrate, forming a trilayer specimen. After drying at 80 °C, the trilayer was placed in a vacuum oven at 170 °C for 240 h. The specimen was cooled to room temperature for the neutron reflectivity measurements. It should be noted that during the transfer onto the surface of existing layers creases or folds in the transferred layer can occur. For the specimens investigated here the occurrence of such defects was minimal, representing much less than 1% of the surface. Since the reflectivity measures an average over the entire surface, these defects will not impair the interpretation of the data and can be ignored. For the investigation of the mixtures of homopolymers and diblock copolymers, solutions of the P(d-S-*b*-MMA) or P(S-*b*-d-MMA) (where the lower case d prior to the block indicates perdeuteration) with the desired amount of d-PS and PMMA or PS and d-PMMA, respectively, were prepared in toluene. The total concentration of the mixture was adjusted to yield the desired film thickness. The solution was then placed on a silicon, Si, substrate and spun at 2×10^3 rpm. The specimens were dried at 80 °C for 20 min and placed in a vacuum oven at 170 °C for 10 days to allow the copolymer mixture to form a multilayered morphology parallel to the surface of the substrate.[11,12,25,26] The specimens were then quenched to room temperature for the reflectivity measurements.

All Si substrates were cleaned in chromic acid, thoroughly rinsed in water, degreased in isopropyl alcohol vapors, and dried. The substrates used for the copolymer mixture study were 10 cm in diameter with a thickness of 5 mm. Those used for the investigation of the homopolymer interface were 5 cm in diameter with a thickness of 5 mm. Thick substrates are required to eliminate bowing of the substrate when mounted in the reflectometer. It should be noted that the cleaning procedure described above will not remove a thin oxide layer on the Si. X-ray reflectivity measurements performed on similar substrates yielded a thickness of the oxide layer of 10–15 Å. The presence of this oxide layer will not be of significant consequence to these studies though.

Some of the neutron reflectivity measurements were performed on the BT-7 diffractometer at the reactor experimental hall of the National Institute of Standards and Technology. The collimated neutron beam from the reactor is monochromated using pyrolytic graphite to obtain neutrons with a wavelength $\lambda = 2.35$ Å. The mosaic spread of the graphite monochromator is 0.667°, yielding $\Delta\lambda/\lambda = 0.01$. Two cadmium slits (0.5 and 0.075 mm separated by ~1.6 m) located before the specimen reduced the angular divergence of the incident beam to ~0.02°. A 1-mm slit (330 mm after the specimen) restricts the acceptance angular of the detector to ~0.18°. A ^{3}He gas-filled detector is used to measure both the incident and reflected beams.

Other neutron reflectometry measurements were performed on the SPEAR instrument at the Manuel Lujan, Jr., Neutron Scattering Center (LANSCE) at the Los Alamos National Laboratory. Because the LANSCE target moderator reflector system is a 20-Hz pulsed source of neutrons, SPEAR is operated as a time-of-flight neutron reflectometer where the neutron's energy (or wavelengths, λ) is determined by its velocity. Thus, a reflection measurement consists of detecting neutrons reflected from the sample as a function of neutron wavelength while maintaining the sample at a fixed angle of incidence, θ, with respect to the incident beam. A typical angle of incidence for these experiments was 1.1° where the incident and reflected beams define a vertical scattering plane. Since SPEAR's frame overlap chopper allows one to choose a neutron wavelength frame of either $1 < \lambda < 16$ Å or $16 < \lambda < 32$ Å, this yields an accessible range of wavevectors (at an incident angle of 1.1°) 0.004 Å$^{-1} < k_{z,0} < 0.12$ Å^{-1} where $k_{z,0} = 2\pi \sin(\theta)/\lambda$. The subscript $z,0$ indicates scattering vectors in the z-direction, normal to the surface, in vacuum, or in air (0). For the current experiments, the short-wavelength frame was all that was necessary. The neutrons are counted by using an Ordela Model 1202N linear position-sensitive neutron detector oriented to detect neutrons in the scattering plane. As defined by the detector resolution, the electronic timing resolution, and the moderator pulse width, the resolution for these experiments varied from $0.03 < \delta k_{z,0}/k_{z,0} < 0.05$ for 0.008 Å$^{-1} < k_{z,0} < 0.06$ Å^{-1}, respectively. With SPEAR for these experiments in this configuration, the minimum measurable reflectivity is ~10^{-6}. Typical counting times were approximately 45 min to obtain the statistics shown in the figures.

Analysis of the reflectivity profile was performed by assuming a scattering length density profile normal to the film surface, dividing this profile into a series of layers forming a histogram, and then using a recursion relationship to calculate the total reflectance. Multiplication by the complex conjugate of the reflectance then yields the reflectivity. Any roughness at the air surface or at the Si interface was explicitly taken into account in the calculation of the reflection coefficient. The standard Debye–Waller correction term was not used. More detailed discussions of the manner in which the reflectivity is calculated can be found elsewhere[17,27-31] and will not be discussed here.

Results and Discussion

The neutron reflectivity profile for a trilayer comprised of a 191-Å-thick film of P(S-*b*-d-MMA) sandwiched between PS and d-PMMA layers is shown in Figure 1. The reflectivity results are shown as a function of the neutron momentum normal to the film surface, $k_{z,0}$. For $k_{z,0} \lesssim 0.0092$ Å^{-1}, corresponding to the critical angle of d-PMMA, the neutrons are totally, externally reflected. As $k_{z,0}$ increases, the reflectivity decreases rapidly, with a single-frequency oscillation in the reflectivity being evident. Analysis and interpretation of the measured reflectivity profile is, by design of the experiment, straightforward. Since the PS or d-MMA segments of the P(S-*b*-d-MMA), at equilibrium, are mixed with the PS or d-MMA homopolymer segments, respectively, then the trilayer specimen reduces, in essence, to a bilayer. The labeling of the homopolymer and copolymer segments is identical, and, consequently, this experiment cannot distinguish between the homopolymer or block copolymer segments. Therefore, the neutrons see only a layer of normal PS segments on top of a layer of d-PMMA segments. In addition, the layer adjacent to the air surface is normal PS, which has a low scattering length density of 1.43×10^{-6} Å^{-2}. This basically means that the reflectance

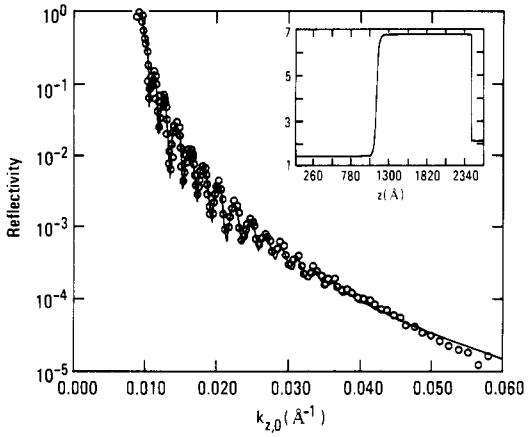

Figure 1. Neutron reflectivity profile for a PS/d-PMMA homopolymer bilayer where a 191-Å layer of P(S-*b*-d-MMA) was placed at the homopolymer interface. The inset shows the scattering length density profile used to calculate the reflectivity profile shown as the solid line. The air/polymer interface corresponds to a z value of zero.

at the air/PS interface is low and the roughness at this interface is of no consequence. In like manner, placing the d-PMMA layer with a scattering length density of 6.8 $\times 10^{-6}$ Å^{-2} adjacent to the Si with a scattering length density of 2.099 $\times 10^{-6}$ Å^{-2} makes the analysis insensitive to the presence of an oxide layer, which would have a scattering length density of 3.48 $\times 10^{-6}$ Å^{-2}. The oxide layer looks effectively as a roughness between the d-PMMA and Si interface.

Analysis of the reflectivity data requires the scattering length densities and thicknesses of the PS and d-PMMA layers and the Si substrate, the roughness between the d-PMMA and Si substrate, and the form of the interface between the PS and d-PMMA layers. The scattering length densities were assumed equal to the bulk values, and the thicknesses were measured independently by optical ellipsometry. The oscillations in the reflectivity profile are due solely to the thickness of the d-PMMA layer, and by measurement of the scattering vector difference between successive minima, $\Delta k_{z,0}$, at high $k_{z,0}$ ($\sim$0.02 Å^{-1}), the thickness of the d-PMMA layer can be directly obtained from $\pi/\Delta k_{z,0}$. The roughness at the d-PMMA/Si interface was determined from independent X-ray and neutron reflectivity measurements of d-PMMA on Si. This was assumed to remain constant for all specimens with an effective width, a_I, as defined below of 20 Å. Variations in this will, of course, introduce errors in the width of the interface between the homopolymers, but this is not of significant consequence. Thus, the only variable or unknown in the analysis is the width of the interface between the PS and d-PMMA layers.

Shown as the solid line in Figure 1 is the reflectivity profile calculated by using the scattering length density profile shown in the inset. The model can be described by a 1126-Å layer of PS on top of a 1305-Å layer of d-PMMA, with an error function describing the width between the PS and d-PMMA. The width of the interface, a_I, defined by the product of the inverse of the slope at the midpoint of the gradient times the scattering length density difference between PS and d-PMMA is 74 ± 4 Å. a_I is related to σ, the standard deviation of the interface from its average value or the typical Debye–Waller parameter by $a_I = 2\sigma$. It should be emphasized that it is impossible to define exactly the functional form of the interface. For example, a hyperbolic tangent function will, also, yield a suitable fit to the data. Linear gradients or squared cosine gradients, though, will not yield adequate agreement with the data.[26] However, the major focus of this work is to evaluate the width of the interface and not attempt an absolute definition of the functional form. By definition, a_I is not sensitive to the functional form of the interface.

Table II
Interfacial Widths

thickness of P(S-*b*-d-MMA) layer,[a] Å	a_I, Å	thickness of P(S-*b*-d-MMA) layer,[a] Å	a_I, Å
0	50 ± 2	239	84 ± 5
80	66 ± 3	341	265 ± 20
85	66 ● 3	372	299 ± 25
191	74 ● 4	∞[b]	50 ± 2

[a] Long period of the P(S-*b*-d-MMA) in the bulk is 512 Å. Consequently, a "monolayer" thickness corresponds to 256 Å. [b] Denotes a pure P(S-*b*-d-MMA) film.

In comparison to the 50 ± 2 Å interfacial width found for PS and PMMA homopolymers or pure P(S-*b*-MMA) diblock copolymers,[25,26] the result of 74 ± 4 Å represents a substantial increase. Therefore, addition of the diblock copolymer to the interface between the PS and d-PMMA results in a broadening of the interfacial width, which is consistent with the expected reduction in the interfacial tension.

Decreasing the thickness of the P(S-*b*-d-MMA) layer between PS and d-PMMA to 85 Å yields a reflectivity profile that is quite similar to that found in Figure 1 and is not shown here. The analysis proceeds as described above, with the result that the interfacial width was found to be smaller at 66 ± 3 Å. This difference of 8 Å is well outside of any errors. It must be kept in mind that reflectivity is most sensitive to the gradient in the scattering length density between the two layers, and, consequently, the precision is quite high.

A compilation of the interfacial widths as a function of the thickness of the P(S-*b*-d-MMA) layer is given in Table II. The result for the PS/d-PMMA homopolymer interface was reported previously.[26] Here it is clearly seen that the addition of the copolymer causes a gradual increase in the width of the interface between the PS and d-PMMA segments.

Up to this point, the thickness of the P(S-*b*-d-MMA) layer between the homopolymers has been kept below 256 Å. This corresponds to half of the lamellar period in the microphase-separated morphology. In a sense this is maintaining a coverage at the interface between the homopolymers at less than a "monolayer" coverage. That is to say, the interface between the PS and d-PMMA has not been saturated with diblock copolymer chains. Increasing the thickness of the P(S-*b*-d-MMA) layer to 341 Å produces rather dramatic changes in the reflectivity profile. Shown in Figure 2 is the reflectivity profile as a function of $k_{z,0}$. Here again the critical angle of the d-PMMA layer is observed at $k_{z,0}$ $\sim$0.0092 Å^{-1}. As $k_{z,0}$ increases, the reflectivity drops rapidly, as would be expected; however, the oscillations characteristic of the d-PMMA layer are rapidly damped. Assuming that the simple bilayer model, used previously, is still applicable here, the reduction in the amplitude of the oscillations would be attributed to a broadening of the interface between the PS and d-PMMA. When the simple bilayer model was used, the scattering length density profile shown in the inset was used to calculate the reflectivity profile shown as the solid line. The agreement between the two profiles is quite good. The surprising feature of the profile is that the width of the interface required to fit the data is 265 ± 20 Å. For the contrast between PS and d-PMMA the reflectivity results show that the interface is quite broad, but the precision to which the interfacial width can be

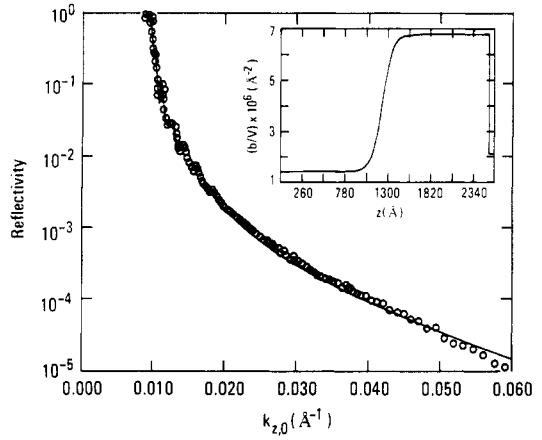

Figure 2. Neutron reflectivity profile for a PS/d-PMMA bilayer where a 341-Å-thick P(S-*b*-d-MMA) layer was placed at the interface. The scattering length density profile shown in the inset was used to calculate the solid line in the figure. As in Figure 1, the position of the air/polymer interface corresponds to zero in the inset.

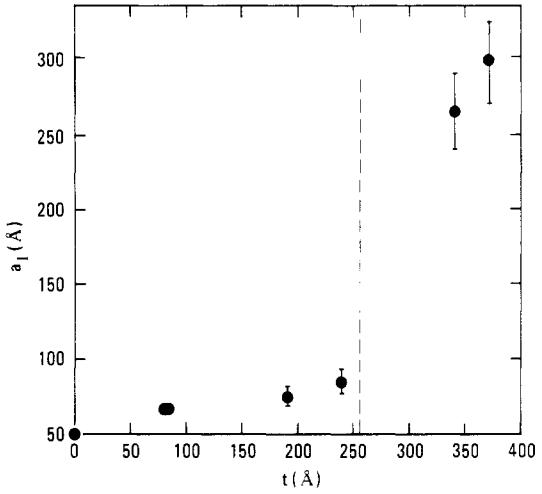

Figure 3. Width of the interface, a_I, between PS and d-PMMA segments as a function of the thickness of the P(S-*b*-d-MMA) layer placed between the two homopolymers. The dashed vertical line corresponds to a thickness of half the period of the lamellar microdomain morphology of P(S-*b*-d-MMA) in the bulk.

determined is low.[32] However, the basic conclusion is clear: that having an excess of the copolymer at the interface results in what appears to be a significant broadening of the interfacial width. A similar result was found for a specimen where the initial thickness of the P(S-*b*-d-MMA) layer was 372 Å. In this case an interfacial width of 299 ± 25 Å was found.

It is instructive to plot the combined set of interfacial widths as a function of the thickness of the initial P(S-*b*-d-MMA) layer between the PS and d-PMMA homopolymer layers. This is shown in Figure 3. As can be seen, a gradual increase in the width of the interface between the PS and d-PMMA segments is seen up to a P(S-*b*-d-MMA) layer thickness of ~256 Å (indicated by the dashed vertical line in the figure). Again, this corresponds to half of the repeat period of the lamellar microdomain morphology in the bulk. Above this value, the interface appears to be saturated and the apparent interfacial width becomes quite large.

It is difficult to believe that the broadening observed with the thicker P(S-*b*-d-MMA) layers characterizes the actual segment density profiles across the interface. In fact, in addition to the specular reflectivity, it is necessary to examine the off-specular scattering where the direction of the scattering vector is not normal to the surface but tilted with respect to the surface normal to an amount commensurate with the measurement angle away from the specular position. In this case, there is a component of the scattering vector in the plane of the film and the measurements become sensitive to lateral correlations in the scattering length density. For the cases where the P(S-*b*-d-MMA) layers were ≲256 Å there was a small amount of off-specular scattering, indicating that there were not pronounced density correlations parallel to the interface.[33,34] This, of course, does not mean that the mixing of the normal and deuterated segments at the interface does not give rise to scattering, only that the magnitude of the scattering was small. However, in cases where the thickness of P(S-*b*-d-MMA) layers was >256 Å, the off-specular scattering increases dramatically. This result can be interpreted in one of at least two ways. First, the presence of the diblock at the interface will reduce the interfacial tension between the PS and d-PMMA and will eventually reach a point where the interfacial tension is zero. At this point, marked curvature at the interface is possible since there is no energy gained by maintaining a planar interface. Since the specular measurements represent the variation in the scattering length density normal to the film surface averaged over the coherence length of the neutrons (~1 μm), then any curvature at the interface that occurs over distance scales less than this would appear as an interfacial broadening. The curvature of the interface would give rise to lateral correlations in the scattering length density and, hence, give rise to the large amount of off-specular scattering. A second possibility is that the interface becomes saturated with the diblock copolymer and micelles are formed at the interface. Shull et al.[24] have observed both for PS/poly(vinyl-2-pyridine), P(V2P), asymmetric diblock copolymers at the interface between PS and P(V2P) homopolymers by electron microscopy. In that study upon examination of bilayers of P(V2P) homopolymers in contact with a mixture of PS with the asymmetric diblock copolymer, micelles are shown to segregate to the interface between the layers, and, in addition, clear evidence is shown for the presence of lateral variations in the composition along the interface. Reflectivity alone cannot distinguish between these different possibilities. Unfortunately, for the case of PS and PMMA under consideration here, attempts to perform similar electron microscopy studies have been unsuccessful due to the sensitivity of PMMA to the electron beam. Nonetheless, the formation of micelles will give rise to a substantial amount of small-angle scattering and hence off-specular scattering. Again, the specular measurements would average over the micelles formed and give the appearance that the interface has broadened substantially. It is not possible, at present, to distinguish between these two possibilities and other possible mechanisms by which a large increase in the lateral density correlations would occur. It is clear though that there is an optimum thickness of the P(S-*b*-d-MMA) layer that will produce a uniform distribution of the copolymer at the interface where the interface is saturated with the diblock. The results here indicate that this occurs for symmetric diblock copolymers at thicknesses of ~$L/2$ where L is the period of the lamellar microdomain morphology. Defining this precisely as $L/2$ is somewhat speculative since the paucity of data points precludes an exact statement. It is clear from the data, though, that it is close to $L/2$.

Studies on the P(S-*b*-d-MMA) and P(d-S-*b*-MMA) copolymer films on Si substrates have quantitatively shown that the width of the interface between the PS and PMMA microdomains is 50 ± 2 Å, identical with that of the PS and PMMA homopolymers.[25,26] Thus, to be consistent with the results shown here, addition of homopolymer to

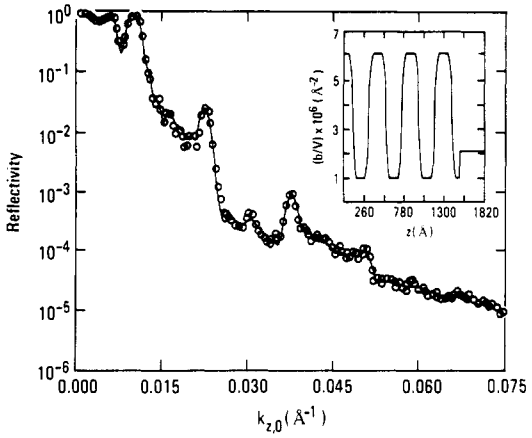

Figure 4. Neutron reflectivity profile for a mixture of 90% P(d-S-*b*-MMA) with 5% d-PS and 4.5% PMMA as a function of the neutron momentum normal to the specimen surface, $k_{z,0}$. The scattering length density profile shown in the inset was used to calculate the solid line in the figure. In the inset, zero corresponds to the air/polymer interface.

the diblock should produce an interfacial broadening. This simply represents the extreme case where the thickness of the copolymer layer is large in comparison to the thickness of the homopolymer layers.

Neutron reflectivity measurements were performed on both P(d-S-*b*-MMA) and P(S-*b*-d-MMA) symmetric diblock copolymers where PS and PMMA homopolymers were mixed with the diblocks. The labeling of the homopolymers and the diblocks was kept the same so that discrimination between the segments of the copolymers and homopolymers was not possible. It should be noted that equal amounts of the PS and PMMA homopolymers with the appropriate labeling were mixed with the copolymer to preserve the lamellar microdomain morphology and to minimize any curvature of the interface between the PS and PMMA microdomains due to an asymmetry in the volume fraction of the components. Independent studies on diblock copolymer mixtures with homopolymers have shown that the multilayered, lamellar morphology parallel to the surface of the Si substrate is maintained and is similar to that seen for the pure diblock copolymers.[35]

The neutron reflectivity profile for the P(d-S-*b*-MMA) symmetric diblock copolymer mixed with 4.5% d-PS and 4.5% PMMA is shown in Figure 4. These data and the corresponding fits typify the results for all the copolymer mixtures. In contrast to the profiles seen for the simple bilayers, the reflectivity profiles for the copolymer mixtures are somewhat more complex. Above the critical angle at least 4 orders of Bragg reflections are seen which characterize the period of the multilayer morphology. Consequently, the variation in the periodicity as a function of the homopolymer composition can be quantitatively determined. The third- and fourth-order reflections are very sensitive to the width of the interface between the d-PS and PMMA microdomains and serve to place tight restrictions on the interfacial widths derived. In addition, a high-frequency oscillation, characteristic of the total thickness of the film, is evident.

The solid line is the reflectivity profile calculated by using the scattering length density profile normal to the film surface shown in the inset. Over the entire scattering vector range the agreement between the calculated and experimental profiles is quite good. As with pure diblock copolymer films, the mixture with the homopolymer shows a preferential segregation of the PS to the air surface and PMMA to the substrate interface. In fact, the thicknesses of the PS and PMMA layer at these two interfaces are half

Table III
Characteristics of Copolymer/Homopolymer Mixtures

copolymer	X_c[a]	X_{PS}[a]	X_{PMMA}[a]	L_{PS},[b] Å	L_{PMMA},[b] Å	a_I, Å
P(S-*b*-d-MMA)	1.0	0	0	268 ± 2	244 ± 2	50 ± 2
P(S-*b*-d-MMA)	0.91	0.045	0.045	291 ± 2	249 ± 2	55 ± 2
P(S-*b*-d-MMA)	0.83	0.085	0.085	308 ± 4	273 ± 4	74 ± 3
P(d-S-*b*-MMA)	1.0	0	0	210 ± 1	188 ± 1	50 ± 2
P(d-S-*b*-MMA)	0.91	0.045	0.045	228 ± 1	209 ± 1	57 ± 2
P(d-S-*b*-MMA)	0.83	0.085	0.085	245 ± 2	227 ± 2	64 ± 3

[a] X_i is the weight fraction of component i where C denotes diblock copolymer and PS or PMMA represent either PS or d-PS and PMMA or d-PMMA. The labeling of the homopolymer corresponds to that of the copolymer; i.e., d-PS and PMMA were mixed with P(d-*b*-MMA). [b] L_i is the thickness of the i component lamellar microdomain.

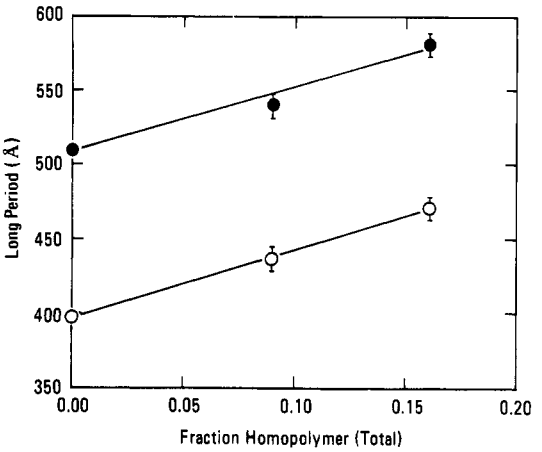

Figure 5. Long period or period of the multilayer for the mixtures of P(d-S-*b*-MMA) with d-PS and PMMA (○) and mixtures of P(S-*b*-d-MMA) with PS and d-PMMA (●) as a function of the total weight fraction of homopolymers. The offset in the period corresponds to the different molecular weights of the copolymers.

the thicknesses of the layers seen in the bulk or, in this case, in the center of the film. This is identical with the result for the pure diblock copolymer films and demonstrates that the addition of 4.5% PS and 4.5% PMMA has not perturbed the ordering of the diblock. The relative thicknesses of the d-PS and PMMA layers are determined by the intensities of the higher order reflections. For example, if the thickness of the d-PS layer was equal to that of the PMMA layer, then, by symmetry, even-order reflections would be absent. The model calculations show that the thickness of the d-PS layer is 228 ± 1 Å and that of the PMMA layer is 209 ± 1 Å. Of major interest, however, is the width of the interface between the d-PS and PMMA layers. For the mixture studied here an interfacial width of 57 ± 2 Å is found, which is 14% larger than that found for the pure copolymer.

The results of similar studies on other mixtures of P(S-*b*-d-MMA) and P(d-S-*b*-MMA) with the appropriate homopolymers are given in Table III. In general, it is seen that the PS and PMMA thicknesses increase with the addition of the homopolymers. Shown in Figure 5 is the long period, i.e., the sum of the PS and PMMA layer thicknesses as a function of the weight fraction of added homopolymer. The variation is essentially linear for both P(S-*b*-d-MMA) and P(d-S-*b*-MMA). The data are displaced from one another due to the difference in the molecular weights of the copolymers, which produces a difference in the period.

The change in the interfacial width is shown in Figure 6 as a function of the weight fraction of homopolymer. What is very clear from these data is that, as homopolymer is added to the copolymer, small amounts of the homopolymer are sufficient to produce a dramatic increase

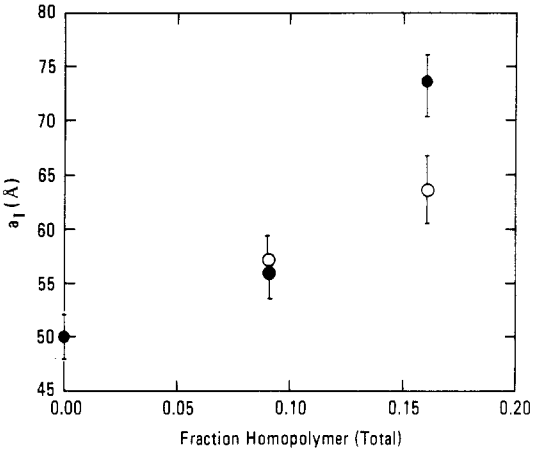

Figure 6. Interfacial widths, a_I, as a function of the total weight fraction of homopolymer added to the diblock copolymer. Results for experiments on both the P(d-S-*b*-MMA) and P(S-*b*-d-MMA) are shown in the figure. The open circles represent data for P(d-S-*b*-MMA) and the filled circles for P(S-*b*-d-MMA).

in the interface width (on the order of 30–50%). Over the concentration range studied the interfacial width continuously increases. Obtaining results at higher homopolymer concentrations is not possible by reflectivity since the orientation of the lamellar microdomains parallel to the surface of the film is lost. Both small-angle X-ray and neutron scattering are insensitive to interfacial widths of the magnitude shown here due to the rapid reduction in the intensity at higher scattering vectors and the inherent problem of subtracting thermal density fluctuation scattering, which is on the same order of magnitude as the coherent scattering of interest. However, in keeping with the results on the addition of the diblock to the interface between the homopolymers, it would be expected that ~85 Å would represent a maximum value and that further addition of homopolymer to the copolymer would not produce any further, substantial broadening.

The results on the copolymer at the interface between the immiscible polymers and those of the homopolymers added to the copolymers indicate that the homopolymers penetrate well into the interfacial region. This has been confirmed in a separate study where the segment density distributions of each component at the interface were evaluated.[23] In fact, if one considers the interface formed between the homopolymers as the probability of finding segments of a given type as a function of distance and similarly for the diblock copolymers where one considers the probability of finding a junction point joining the two blocks, then the results shown here suggest that the interfacial width for homopolymers in the presence of symmetric diblock copolymers is, effectively, a convolution of the two segment density distributions at the interface, thereby giving rise to a broader interface. As mentioned earlier, the broadening of the interface is, also, consistent with the reduction in the interfacial tension between the two components.

In conclusion, it has been shown that the addition of a diblock copolymer to the interface between immiscible homopolymers results in a broadening of the interfacial width. The interfacial width increases up to a point where saturation of the interface with the diblock copolymer occurs. This corresponds to approximately half of the long period of the lamellar microdomain morphology in the bulk, which can be viewed as essentially a "monolayer" of the diblock copolymer. At higher copolymer concentrations either the interface exhibits marked curvature or micelles are formed at the interface. Examination of the off-specular scattering is in progress to distinguish between these different possibilities. Similarly, as homopolymer is added to the diblock copolymers, the interfacial width between the lamellar microdomains increases as a function of composition and approaches the width found for the addition of copolymer to the interface between immiscible homopolymers.

Acknowledgment. This work was partially supported by the United States Department of Energy, Office of Basic Energy Sciences, Grant No. FG03-88ER 45375. This work benefitted from the use of SPEAR at the Manuel P. Lujan, Jr., Neutron Scattering Center at the Los Alamos National Laboratory, which is supported by the United States Department of Energy, Office of Basic Energy Sciences, and other Department of Energy programs under Contact No. W-7405-ENG-32 to the University of California.

References and Notes

(1) Helfand, E.; Wasseman, Z. R. In *Developments in Block Copolymers. 1*; Goodman, I., Ed.; Applied Science Publishing: New York, 1982.
(2) Wu, S. *Polymer Interface and Adhesion*; Marcel Dekker, Inc.: New York, 1982.
(3) Sanchez, I. C. *Annu. Rev. Mater. Sci.* **1983**, *13*, 387.
(4) Poser, C. I.; Sanchez, I. C. *Macromolecules* **1981**, *14*, 361.
(5) Noolandi, J.; Hong, K. M. *Macromolecules* **1982**, *15*, 482.
(6) Noolandi, J.; Hong, K. M. *Macromolecules* **1984**, *17*, 1531.
(7) Helfand, E.; Bhattacharjee, S. M.; Fredrickson, G. H. *J. Chem. Phys.* **1989**, *91*, 7200.
(8) Leibler, L. *Macromolecules* **1982**, *15*, 1283.
(9) Vilgis, T. A.; Borsali, R. *Macromolecules* **1990**, *23*, 3172.
(10) Leibler, L. *Macromol. Chem., Macromol. Symp.* **1988**, *16*, 1.
(11) Coulon, G.; Russell, T. P.; Deline, V. R.; Green, P. F. *Macromolecules* **1989**, *22*, 2581.
(12) Russell, T. P.; Coulon, G.; Deline, V. R.; Miller, D. C. *Macromolecules* **1989**, *22*, 2581.
(13) Whitlow, S. J.; Wool, R. P. *Macromolecules* **1989**, *22*, 2648.
(14) Russell, T. P.; Karim, A.; Mansour, A.; Felcher, G. P. *Macromolecules* **1988**, *21*, 1890.
(15) Fernandez, M. L.; Higgins, J. S.; Penfold, J.; Ward, R. C.; Shackleton, C.; Walsh, D. J. *Polymer* **1988**, *29*, 1923.
(16) Stamm, M.; Majkrzak, G. F. *Polym. Prepr. (Am. Chem. Soc., Div. Polym. Sci.)* **1987**, *28*, 18.
(17) Russell, T. P. *Mater. Sci. Rep.* **1990**, *5*, 171.
(18) Brown, H. R. *Macromolecules* **1989**, *22*, 2859.
(19) Fayt, R.; Jérôme, R.; Teyssie, Ph. *J. Polym. Sci., Polym. Lett.* **1986**, *24*, 25.
(20) Shull, K. R.; Kramer, E. J.; Hadziioannou, G.; Tang, W. *Macromolecules* **1990**, *23*, 4780.
(21) Wakharhar, V. S.; Deline, V. R.; Russell, T. P. *SIMS VII* **1990**, 363.
(22) Brown, H. R.; Char, K.; Deline, V. R. *Macromolecules* **1990**, *23*, 3383.
(23) Russell, T. P.; Anastasiadis, S. H.; Menelle, A.; Felcher, G. P.; Satija, S. K. *Macromolecules* **1991**, *24*, 1575.
(24) Shull, K. R.; Winey, K. I.; Thomas, E. L.; Kramer, E. J. *Macromolecules* **1991**, *24*, 2748.
(25) Anastasiadis, S. H.; Russell, T. P.; Satija, S. K.; Majkrzak, C. F. *Phys. Rev. Lett.* **1989**, *62*, 1852.
(26) Anastasiadis, S. H.; Russell, T. P.; Satija, S. K.; Majkrzak, C. F. *J. Chem. Phys.* **1990**, *92*, 5677.
(27) Werner, S. A.; Klein, A. G. *Neutron Scattering*; Price, D. I., Skold, K., Eds.; Academic Press: New York, 1989.
(28) Heavens, O. S. *Optical Properties of Thin Solid Films*; Dover Publishing: New York, 1965.
(29) Parrat, L. G. *Phys. Rev.* **1954**, *54*, 359.
(30) Als-Nielsen, J. In *Structure and Dynamics of Surfaces II*; Schommers, M., von Blanckenhagen, P., Eds.; Springer-Verlag: Berlin, 1987.
(31) Lekner, J. *Theory of Reflection*; Nijhoff: Dordrecht, The Netherlands, 1987.
(32) Karim, A.; Mansour, A.; Felcher, G. P.; Russell, T. P. *Mater. Res. Soc. Symp.* **1990**, *171*, 329.
(33) Sinha, S. K.; Sirota, E. B.; Garoff, S.; Stanley, H. B. *Phys. Rev. B* **1988**, *38*, 2297.
(34) Pynn, R., to be published.
(35) Russell, T. P.; Anastasiadis, S. H.; Satija, S. K.; Majkrzak, C. F., unpublished results.

Registry No. PMMA, 9011-14-7; PS, 9003-53-6; P(S-*b*-MMA), 106911-77-7.